Entropy **2012**, *14*, 533-558; doi:10.3390/e14030533

OPEN ACCESS

entropy

ISSN 1099-4300

www.mdpi.com/journal/entropy

Article

Curvature Entropy for Curved Profile Generation

Yoshiki Ujiie, Takeo Kato, Koichiro Sato * and Yoshiyuki Matsuoka

Department of Mechanical Engineering, Keio University, 3-14-1 Hiyoshi, Kohoku-ku, Yokohama, 223-8522, Japan; E-Mails: ujiie@mech.keio.ac.jp (Y.U.); kato@mech.keio.ac.jp (T.K.); matsuoka@mech.keio.ac.jp (Y.M.)

* Author to whom correspondence should be addressed; E-Mail: koichiro_sato@a3.keio.jp.

Received: 20 December 2011; in revised form: 28 February 2012 / Accepted: 6 March 2012 / Published: 9 March 2012

Abstract: In a curved surface design, the overall shape features that emerge from combinations of shape elements are important. However, controlling the features of the overall shape in curved profiles is difficult using conventional microscopic shape information such as dimension. Herein two types of macroscopic shape information, curvature entropy and quadrature curvature entropy, quantitatively represent the features of the overall shape. The curvature entropy is calculated by the curvature distribution, and represents the complexity of a shape (one of the overall shape features). The quadrature curvature entropy is an improvement of the curvature entropy by introducing a Markov process to evaluate the continuity of a curvature and to approximate human cognition of the shape. Additionally, a shape generation method using a genetic algorithm as a calculator and the entropy as a shape generation index is presented. Finally, the applicability of the proposed method is demonstrated using the side view of an automobile as a design example.

Keywords: curves; information theory; shape generation

---

1. Introduction

In curved surface designs, the overall shape features that emerge due to combinations of shape elements are important because humans tend to perceive the overall shape features macroscopically [1–5]. Unfortunately, controlling the overall shape features in curved profiles is difficult using conventional microscopic shape information, such as dimension, and consequently depends on the experience and intuition of the designers. In studies on microscopic shape information, shapes have been classified quantitatively using microscopic shape information [6], but the relationship between microscopic shape information and macroscopic features remains unclear. On the other hand, research on the representation of a curved line shape has proposed a method for pattern matching, which is robust for changes in rotation and scale [7–10], but the relationship between representation and macroscopic features has not been discussed. Although research on the relationship between curvature, which is utilized as representation, and cognition has been conducted [11–13], in previous works the relationship between curvature and macroscopic features generated by combination of curve segments has not been clarified. Therefore, in curved surface designs, a design support system to represent the overall shape features from macroscopic shape information is desired.

The objective of this study is to propose macroscopic shape information to represent the overall shape features in curved profiles and to confirm its effectiveness. Section 2 describes the proposed entropy as macroscopic shape information of a curved profile. In previous research on the texture and pattern of the cell structure [14,15], entropy in information theory has been used as an index to represent macroscopic features. Herein the concept of entropy is improved to represent the macroscopic features of curves. Section 3 describes the characteristic analyses of the shape information, including the proposed entropy, while Section 4 improves the proposed entropy in an effort to evaluate the continuity of a curve and to analyze the difference between the two proposed entropies. Based on our previous study [16], Section 5 describes a shape generation method using a genetic algorithm and the entropy as a calculator and shape generation index, respectively. Then to examine the availability of the method and index, this method is applied to the side view design of an automobile, which is expressed by a three-dimensional Bézier curve, and a cognition experiment using the generated shapes is conducted to confirm if the entropy adequately represents the cognition information.

2. Definition of Macroscopic Shape Information

In information theory, the information source outputs a series of source symbols [17,18]. The information content I_τ is defined using the occurrence probability of source symbol s_τ in a series of source symbols p_τ as:

$$I_\tau = -\log_2 p_\tau \qquad (p_\tau = P[s_\tau]) \tag{1}$$

where $P[A]$ is the feasibility of event A occurring.

The average information content H is a measure of the average uncertainty and is defined as:

$$H = \sum_{\tau=1}^{A} p_\tau I_\tau = -\sum_{\tau=1}^{A} p_\tau \log_2 p_\tau \tag{2}$$

where A is the number of the source symbols. In information theory, H is called entropy because the equation is identical to that used in thermodynamics. In the present study, a curved line is assumed to be the information source, and the macroscopic shape information is the entropy, expected angle variation, and curvature variation of the curve. These values are described below.

2.1. Angle Variation

The entropy and expected angle variation are calculated in the following manner. First, a curved profile is divided by sampling points into N equivalent curve units (Figure 1a), and the angle variation in each curve unit φ_n is calculated (Figure 1b). N is assumed to be 25, 50, 100, 200, or 400. Each angle variation φ_n corresponds to source symbol s_g, and a series of source symbols is constructed. As shown in Figure 1c, the range of angle variation is set from 0 to 180 degrees in one degree increments (*i.e.*, the number of source symbols T is set to 180). Finally, the occurrence probability of source symbol p_g is calculated (Figure 1d). The angle entropy H_A is calculated using the following equations:

$$H_A = -\frac{1}{\log_2 T} \sum_{g=1}^{T} p_g \log_2 p_g \qquad (0 \le H_A \le 1) \tag{3}$$

To ensure that the variation range is between 0 and 1, H_A is divided by the maximum entropy $\log_2 T$.

Figure 1. Extraction of the angle variation distribution. (**a**) Sampling point and a curve unit; (**b**) Sampling of the angle variation; (**c**) Quantization based on the angle variation; (**d**) Calculation of the occurrence probability.

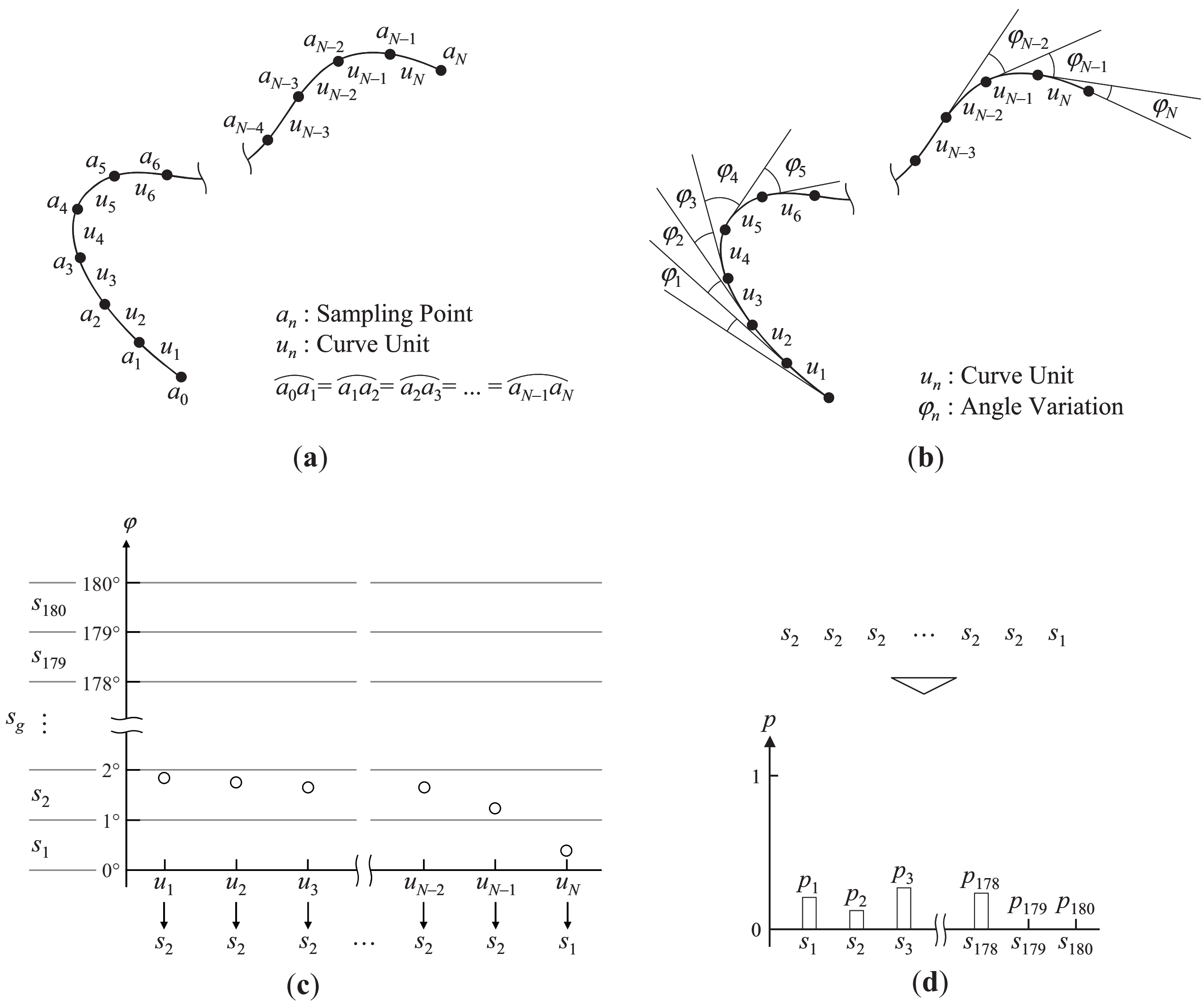

Source symbol s_g corresponds to φ_{Sg} (the angle variation at source symbol s_g) according to the following equation:

$$\varphi_{S_g} = \frac{2g-1}{2} \tag{4}$$

Thus, the expected angle value (the expected angle variation) E_A is calculated as:

$$E_A = \sum_{g=1}^{T} p_g \varphi_{S_g} \tag{5}$$

2.2. Curvature Variation

Entropy and the expected curvature variation are calculated using the following procedure. First, the curved profile is divided by sampling points into N equivalent curve units to curvature ρ (Figure 2a). Then the curvature variation in each curve unit $\Delta\rho_n$ is calculated (Figure 2b) as:

$$\Delta\rho_n = \left\| \rho_n \right| - \left| \rho_{n-1} \right\| \tag{6}$$

Each curvature variation $\Delta\rho_n$ corresponds to the source symbol s_h, and a series of source symbols is constructed. In reference to a conventional study [11–13], the range of log10($\Delta\rho_n$ L) is set from −2 to 3 where L is the total length of a curved profile, while the number of source symbols U is set to 100 (Figure 2c). Finally, the occurrence probability of source symbol p_h is set (Figure 2d). The curvature entropy H_C is calculated using the following equation:

$$H_C = -\frac{1}{\log_2 U} \sum_{h=1}^{U} p_h \log_2 p_h \qquad (0 \le H_C \le 1) \tag{7}$$

H_C is divided by the maximum entropy for the same reason as the angle entropy.

Source symbol s_h corresponds to $\Delta\rho_{Sh}$ (the curvature variation at source symbol s_h), which is expressed as:

$$\Delta\rho_{S_h} = \frac{10^{0.05(h-1)-1.975}}{L} \tag{8}$$

Then, the expected curvature value (the curvature variation) E_C is calculated as:

$$E_C = \sum_{h=1}^{U} p_h \Delta\rho_{S_h} \tag{9}$$

For example, when a very small interval is used to calculate the index of the shape described in Figure 3, the proposed index increases upon changing the microscopic curvature in Figure 3a. Although the shape in Figure 3b has the same macroscopic features, the index greatly differs. Therefore, the points should be set at adequate intervals after considering the influence of noise. Incidentally, we have conducted a study on the removal of this influence [19].

Figure 2. Extraction of the curvature variation distribution. (**a**) Sampling point and a curve unit; (**b**) Sampling of the curvature variation; (**c**) Quantization based on the curvature variation; (**d**) Calculation of the occurrence probability.

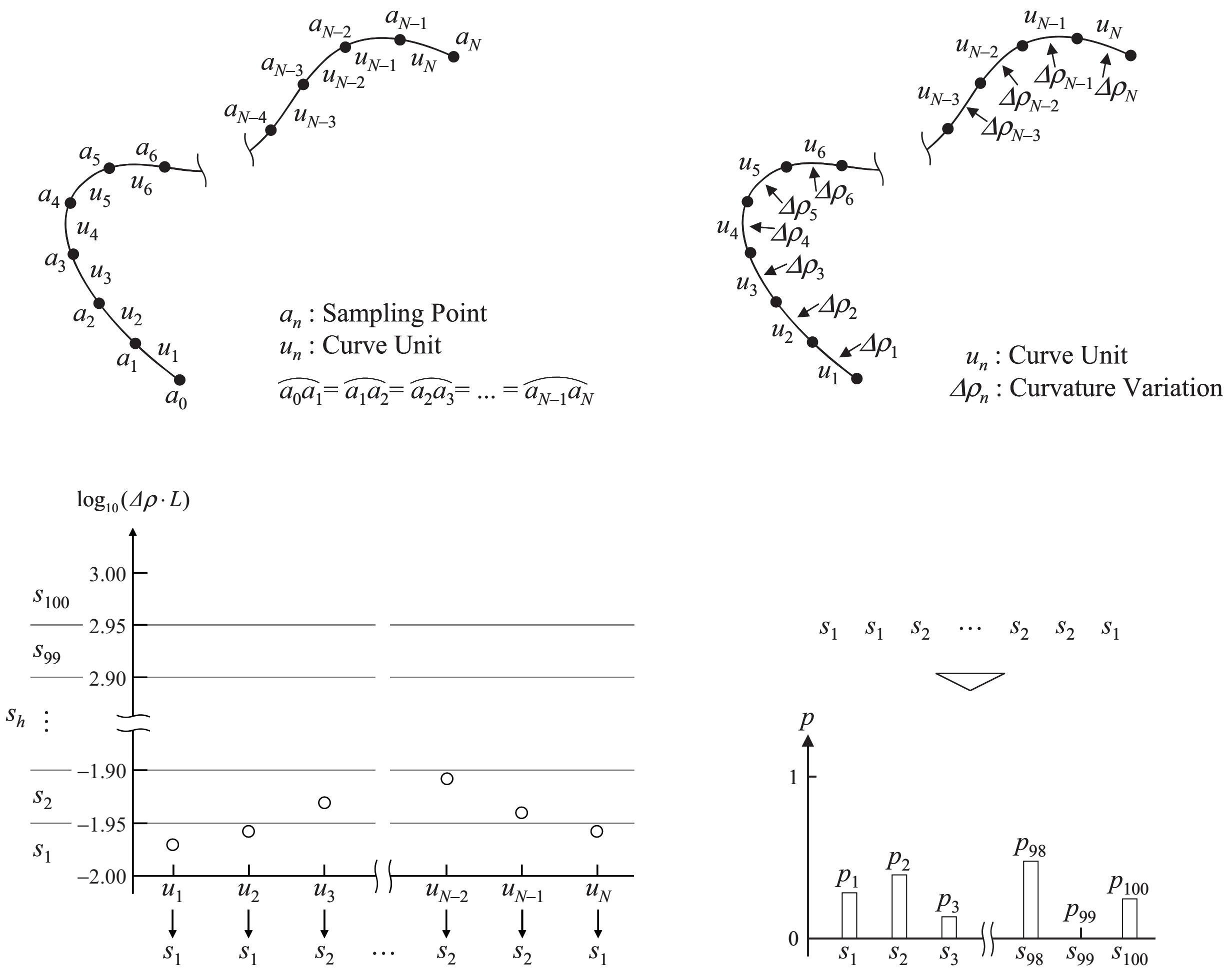

Figure 3. Influence of noise. (**a**) Large variation in the curvature; (**b**) Small variation in the curvature.

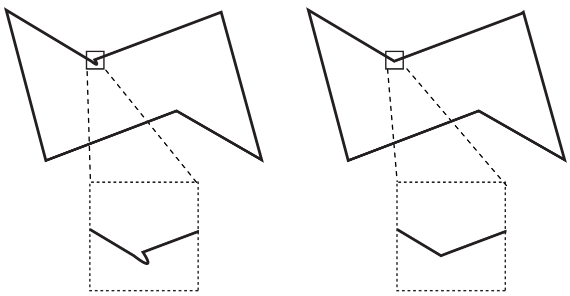

(**a**) (**b**)

3. Characteristic Analysis of Shape Information in Basic Curved Profiles

3.1. Description of Basic Curved Profiles

To create basic curved profiles based on standard polygonal profiles, we selected some polygonal profiles from the 90 polygonal profiles used in the "Aesthetic Measure" by Birkhoff, who is a pioneer in employing an experimental psychology approach in the field of "aesthetics" [20]. We classified 90 polygonal profiles on the basis of similarity, and extracted 20 polygonal profiles to represent each similarly shaped group using the KJ method [21] (Figure 4). Among the 20 polygonal profiles, cluster analysis in which the microscopic shape information is used as a variable, is performed. Table 1 shows the microscopic shape information used in the analysis. This information can be applied to curved profiles and serve as variables for quantitative classification in a conventional study [6]. Consequently, the polygonal profiles are classified into three clusters (Figure 5). We selected shapes 2, 13, and 17 as basic polygonal profiles (Figure 6).

In the present study, a three-dimensional Bézier curve is used to describe basic curved profiles. Various curved profiles can be constructed by connecting several three-dimensional Bézier curves [22,23]. As illustrated in Figure 7, P_0 and P_3 are defined as connection points, P_1 and P_2 are defined as control points, and $\overrightarrow{P_0P_1}$ and $\overrightarrow{P_3P_2}$ are defined as tangent vectors. The position of the connection point, the direction of a tangent vector, and the size of a tangent vector are defined as curve control variables.

Figure 4. Polygonal profiles.

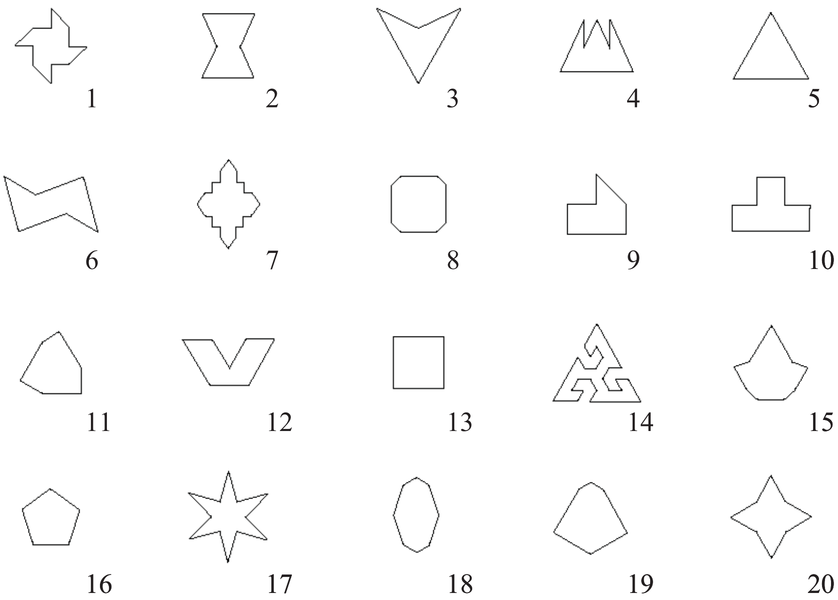

Table 1. Microscopic shape information.

1. Circumference	6. Average width
2. Area	7. Inclusiveness length
3. X maximum width	8. Maximum radius vector
4. Y maximum width	9. Minimum radius vector
5. Roundness	10. Average radius vector

Figure 5. Cluster analysis result.

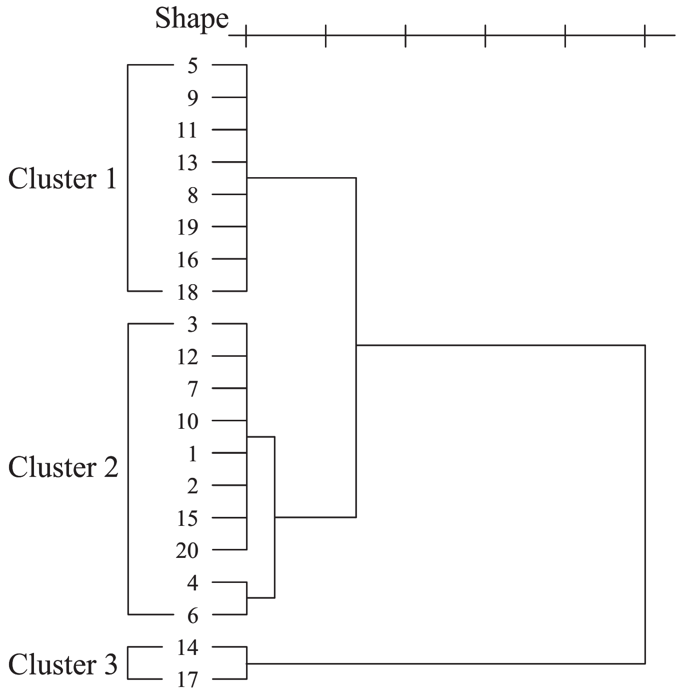

Figure 6. Basic polygonal profiles.

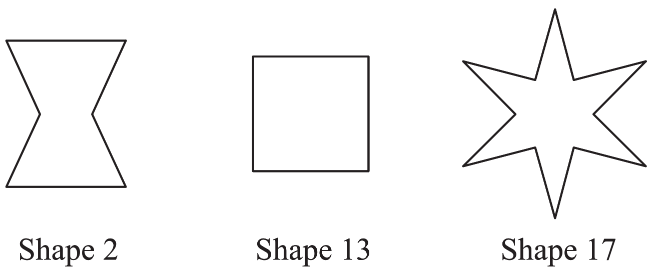

Figure 7. Illustration of a three-dimensional Bézier curve.

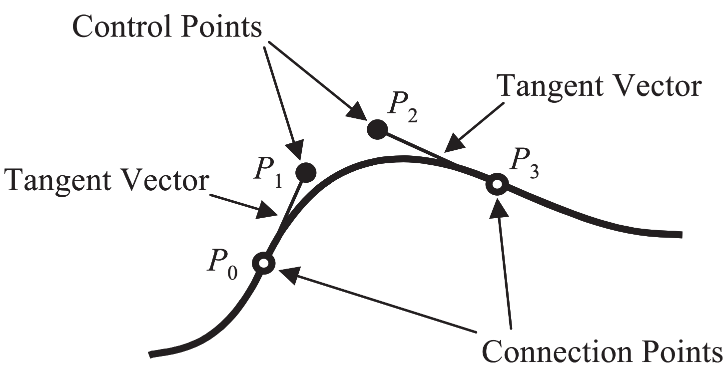

The general equation of a three-dimensional Bézier curve can be expressed as:

$$\boldsymbol{P}(t) = (1-t)^3 \boldsymbol{P}_0 + 3(1-t)^2 t\boldsymbol{P}_1 + 3(1-t)t^2 \boldsymbol{P}_2 + t^3 \boldsymbol{P}_3 \tag{10}$$

where $\boldsymbol{P}_i$ is a position vector of point P_i.

A condition to describe a smooth curved profile is necessary when the curved profile is expressed as a connection of several curve segments. The condition is defined such that $P_3(Q_0)$ is located on P_2 Q_1, as shown in Figure 8. In other words, a three-dimensional Bézier curve with a continuous and differentiable connection point satisfies the following equation:

$$\boldsymbol{Q}_0\boldsymbol{Q}_1 = -m\boldsymbol{P}_3\boldsymbol{P}_2 \qquad (m > 0) \tag{11}$$

Figure 8. Connection of a three-dimensional Bézier curve.

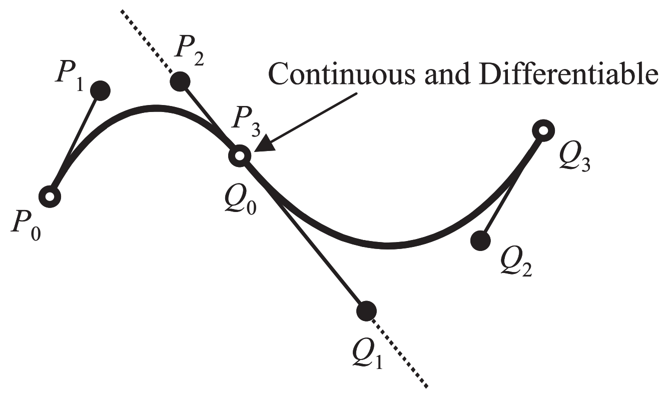

Figure 9 shows a method to express a basic curved profile by a three-dimensional Bézier curve. First, circles with radii r_1 through r_7 are drawn to select the positions of the connection points. The intersection points between the edges of the circles and the polygonal profile J_1 thorough J_{12} are assumed to be the connection points. To improve the smoothness of a curved profile, radii r_1 through r_7 are defined as:

$$\begin{cases} r_1 = \dfrac{1}{4}\min\left\{ \overline{F_6F_1},\ \overline{F_1F_2} \right\} \\ r_k = \dfrac{1}{4}\min\left\{ \overline{F_{k-1}F_k},\ \overline{F_kF_{k+1}} \right\} \ (k = 2,3,4,5) \\ r_6 = \dfrac{1}{4}\min\left\{ \overline{F_5F_6},\ \overline{F_6F_1} \right\} \end{cases} \tag{12}$$

Then each segment J_1 J_2 through J_{12} J_1 is interpolated by a three-dimensional Bézier curve (Figure 9). Considering the continuity of the curve, the size of each tangent vector λ is set to 1/3 of the interval length of the connection point, and using the tangent vector size, the positions of control points C_1 through C_{24} are preliminarily set on the polygonal profile. When the direction of a tangent vector changes, the two tangent vectors always satisfy Equation (11).

Changes in the direction and the size of the tangent vector are defined as the parameters to generate the profiles, and the number of their level is set to five. Therefore, as shown in Figure 10, 25 curved profiles are made from each basic polygonal profile. To prevent the curved profile from possessing both a cross point and a nondifferentiable point, the parameter for the directional change of the tangent vector A_n and the parameter for the size change of the tangent vector L_e are defined in the following equations:

$$
\begin{aligned}
A_n &= \left\{-\frac{1}{4}\theta,\ -\frac{1}{8}\theta,\ 0,\ \frac{1}{8}\theta,\ \frac{1}{4}\theta\right\} \\
L_e &= \left\{\frac{1}{3}\lambda,\ \frac{1}{2}\lambda,\ \lambda,\ \frac{3}{2}\lambda,\ 2\lambda\right\}
\end{aligned}
\tag{13}
$$

where θ is the angle at the top of the polygonal line that connects basic points and λ is the size of the basic tangent vector.

Figure 9. Description of a curved profile.

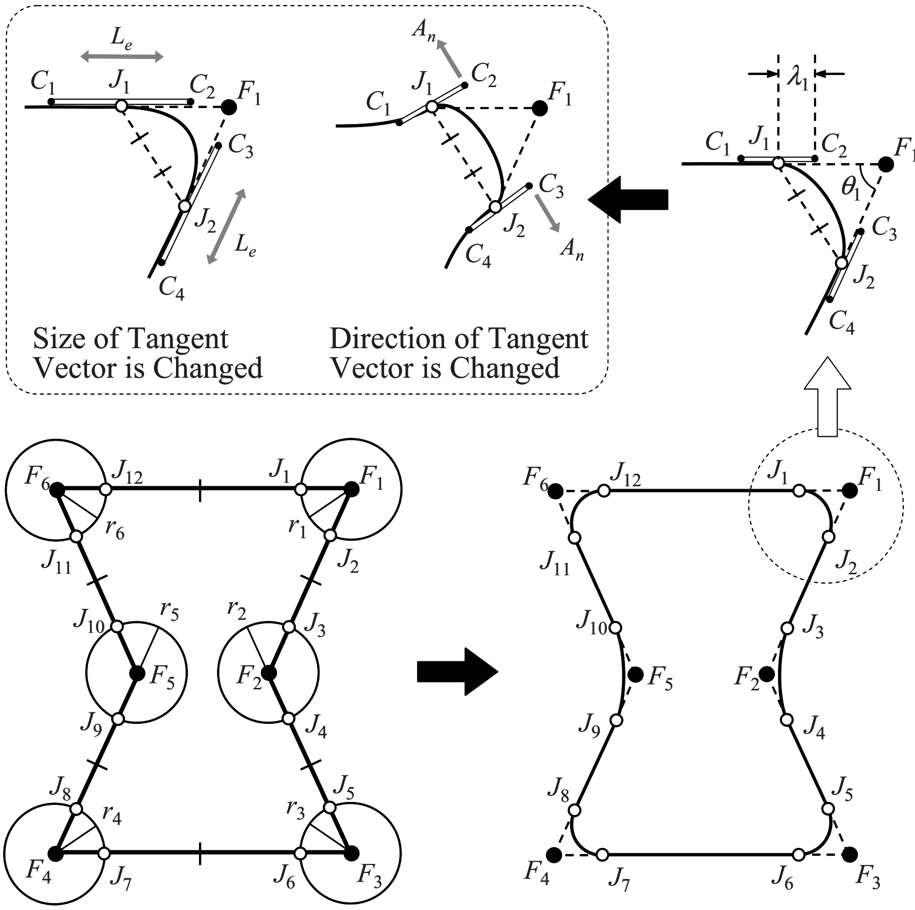

Figure 10. Basic curved profiles. (**a**) Curved profiles based on shape 2; (**b**) Curved profiles based on shape 13; (**c**) Curved profiles based on shape 17.

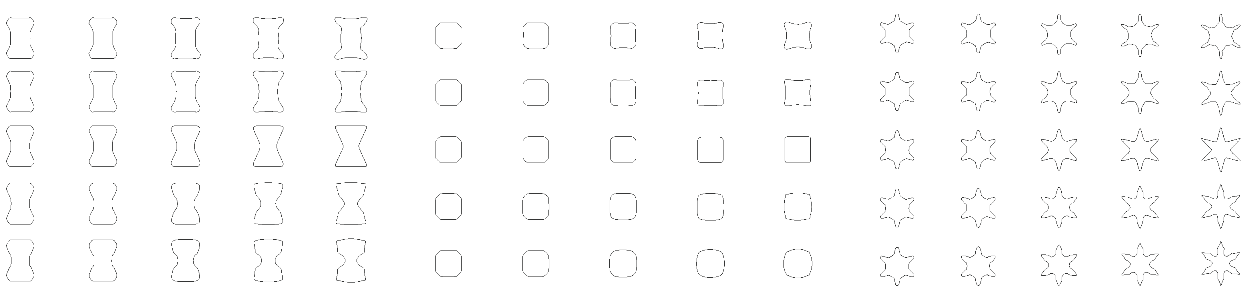

(**a**) (**b**) (**c**)

3.2. Cognition Experiment of the Curved Profile

To analyze the relationship between shape information and cognition information of a curved profile, we implemented a cognition experiment. Cognition information, which is an evaluation value of the macroscopic features, is derived using the semantic differential method. The cognition experiment is performed as follows:

(1) Method: semantic differential method (7 stages)
(2) Samples: 75 samples (basic curved profiles shown in Figure 10)
(3) Evaluation items: 6 items (refer to Table 2)
(4) Examinees: 12 students in their early 20s

According to our previous study [24], six evaluation items are important to represent the macroscopic features in a curved profile. Figure 10 shows the samples displayed on a PC monitor.

Table 2. Evaluation items.

1. Complex	4. Light
2. Rectilinear	5. Fresh
3. Beautiful	6. Hard

3.3. Analysis

3.3.1. Relationship between Microscopic and Macroscopic Shape Information

The relationship between microscopic (conventional) and macroscopic (proposed) shape information in the curved profile is analyzed. To classify the shape information characteristics, each shape information value of the basic curved profile (Figure 10) is calculated and analyzed using principal component analysis as follows. First, the values of shape information, which includes the microscopic shape information shown in Table 1, angle entropy, and curvature entropy, are calculated according to the 75 basic shapes. Next, the values are divided by the value of each basic shape to derive the variance-covariance matrix. Finally, the principal component (eigenvector) and contribution ratio are calculated from the matrix (Table 3). The angle entropy and expected angle value are effective in the first principal component. The curvature entropy and expected curvature value, are effective in the third principal component, and are independent of other shape information. Consequently, macroscopic shape information, which is calculated by the distribution of curvature variation, may have characteristics that differ from the microscopic shape information.

Table 3. Principal components of shape information.

Shape-information	**1st principal component**	**2nd principal component**	**3rd principal component**	**4th principal component**	**5th principal component**
Maximum radius vector	**0.981**	0.065	−0.028	−0.065	−0.106
Inclusiveness length	**0.954**	0.229	−0.052	−0.103	−0.130
Angle expected value	**−0.950**	−0.219	0.136	0.119	0.027
Circumference	**−0.947**	−0.181	0.060	−0.108	0.021
Average width	**0.846**	0.502	−0.081	−0.090	0.006
Roundness	**0.829**	0.524	−0.099	−0.073	−0.042
Angle entropy	**−0.786**	−0.408	0.352	0.020	−0.073
X maximum width	0.265	**0.913**	−0.099	0.208	0.185
Minimum radius vector	0.435	**0.863**	−0.112	0.194	0.075
Y maximum width	0.430	**0.685**	−0.022	−0.452	0.254
Curvature expected value	0.058	−0.074	**−0.963**	−0.127	−0.066
Curvature entropy	−0.182	−0.271	**0.910**	−0.082	−0.034
Average radius vector	−0.075	0.161	0.053	**0.937**	0.242
Area	−0.165	0.223	0.036	0.223	**0.928**
Contribution ratio (%)	57.5	16.1	12.3	7.0	3.9
Accumulation contribution ratio (%)	57.5	73.6	85.9	92.9	96.8

3.3.2. Relationship between the Tangent Vector and Shape Information

The relationship between shape information and the changes in size and direction of the tangent vector in curved profiles is analyzed. We performed a multiple regression analysis in which the changes in the size and direction of the tangent vector are explanatory variables, and the shape information is set as a variable (Figure 11). The multiple correlation coefficient exceeds 0.8 for all of the purpose variables, which have significance levels below 1%. Moreover, for the microscopic shape information, the standard partial regression coefficient for the change in the size of tangent vector (C_{Le}) tends to be larger than that for the change in the direction of tangent vector (C_{An}). On the other hand, for the macroscopic shape information, C_{An} tends to be larger than C_{Le}. Consequently, as mentioned in Section 3.3.1, macroscopic shape information differs from the microscopic shape information in basic curved profiles.

3.3.3. Relationship between Shape Information and Cognition Information

The relationship between shape information and cognition information in curved profiles is analyzed using multiple regression analysis. In the analysis, evaluation items are set as purpose variables, and the five principal components in shape information are set as explanatory variables. The multiple correlation coefficient exceeds 0.7 for the evaluation item of “complex”, but the coefficients of the other items are less than 0.7 (Figure 12).

Figure 11. Standard partial regression coefficient of shape information.

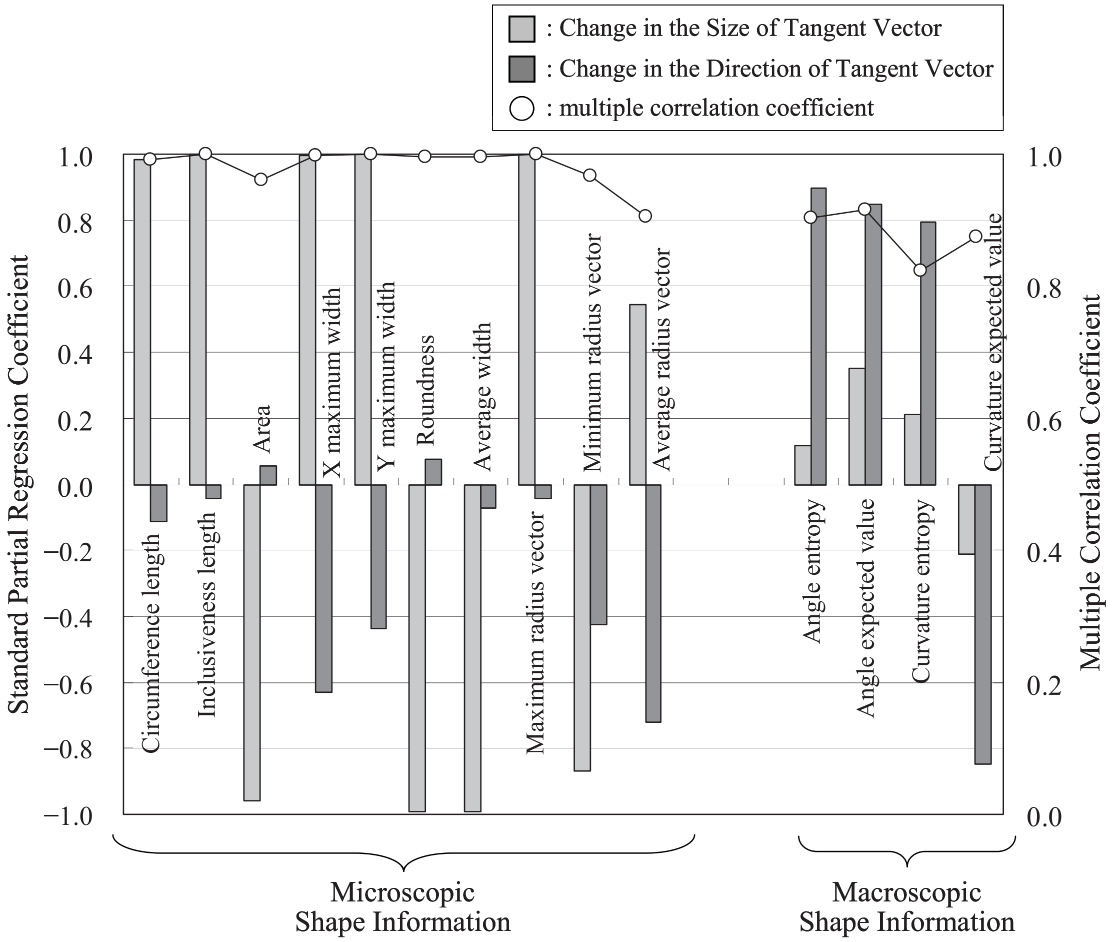

Figure 12. Standard partial regression coefficient of the principle component.

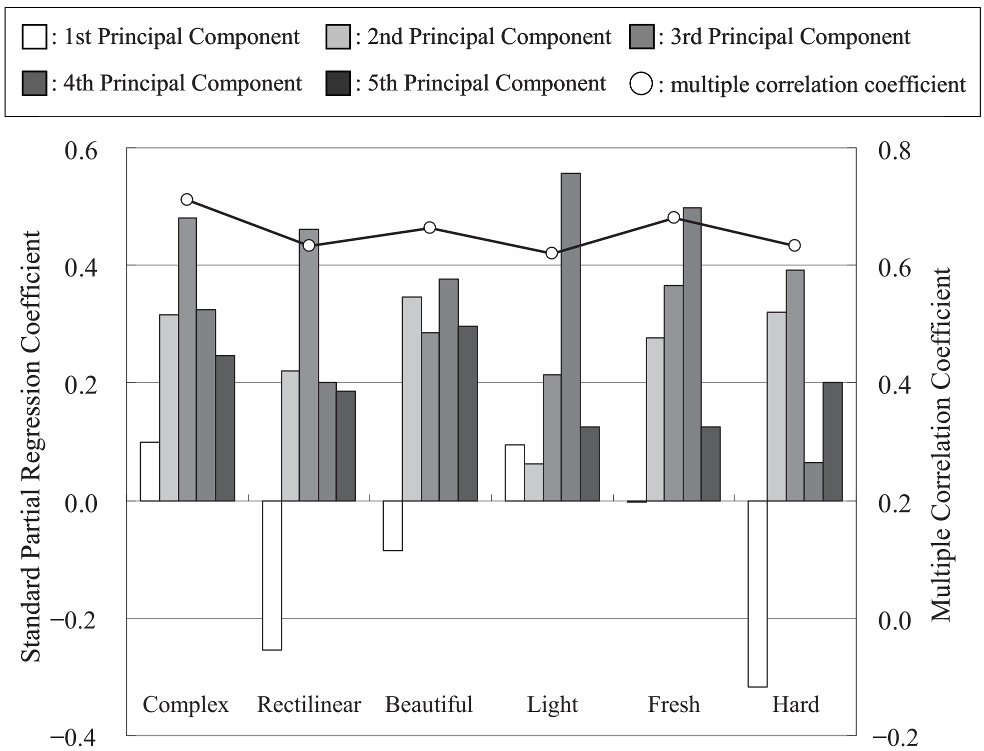

The levels of significance are less than 0.01. Moreover, the standard partial regression coefficient of the third principal component (Table 3) is approximately 0.5 for the "complex" evaluation item, but is higher for the other items. Consequently, the macroscopic shape information is confirmed to represent the complexity of a shape, which is the feature of the overall shape in basic curved profiles.

4. Improvement of the Macroscopic Shape Information

In conventional research on human cognition of a curve segment [11], the relationship between the change process in the curvature and cognition is suggested. This means humans can recognize not only the curvature but also the linkage of curvature. To consider the change process in the curvature, the proposed curvature entropy is improved by introducing a Markov process. An improved curvature entropy has the potential to adequately represent macroscopic shape information based on human cognition.

4.1. Definition of the Quadratic Curvature Entropy

In an actual series of source symbols such as sentences, the connection between source symbols is often constrained [17,18]. In such cases the occurrence probability of a source symbol is the transition probability, which depends on the previous state (or the previous series of source symbols). This stochastic process is called a Markov process. The information source to generate such a series of source symbols is called a Markov source. Information content $I_{\nu,\tau}$ is defined as:

$$I_{\nu,\tau} = -\log_2 q_{\nu,\tau} \quad \left(q_{\nu,\tau} = P[s_\tau | s_\nu]\right) \tag{14}$$

where s_τ and s_ν are source symbols and $q_{\nu,\tau}$ is the transition probability that a source symbol transits from s_τ to s_ν.

The entropy in a Markov source is defined as:

$$H_m = \sum_{\nu=1}^{\Lambda^\delta} \sum_{\tau=1}^{\Lambda} q_\nu q_{\nu,\tau} I_{\nu,\tau} = -\sum_{\nu=1}^{\Lambda^\delta} \sum_{\tau=1}^{\Lambda} q_\nu q_{\nu,\tau} \log_2 q_{\nu,\tau} \tag{15}$$

where q_ν is the occurrence probability of a state, δ is the number of the source symbols within a state, and Λ is the number of source symbol types. A curved line is assumed to be a Markov source, and the macroscopic shape information (curvature entropy based on the Markov process) is calculated in the following manner. First, a curved profile is divided by sampling points into N equivalent curve units (Figure 13a), and the curvature ρ_n in each sampling point is calculated (Figure 13b). Next, the curvature ρ_n is divided by the standard deviation of curvature σ, and the values (ρ_n/σ) correspond to source symbol s_j in order to construct a series of source symbols. Then, as illustrated in Figure 13c, the range of ρ_n/σ, for example, is set from −1.5 to 1.5, and the number of source symbols V is eight. Finally, q_i (the occurrence probability of state S_i) and $q_{i,j}$ (the transition probability of state S_i to source symbol s_j) are set (Figure 13d). d denotes the number of source symbols that constitute a state, and in this study is set to one. The curvature range, number of correspondence source symbols, and number of source symbols that constitute a state are assumed to be parameters and are set to specific levels so the curvature entropy is highly correlated with the complexity of the basic curved profiles. According to information theory, the above-mentioned entropy is called quadratic entropy. The quadratic curvature entropy H_{QC} is calculated using the following equation:

$$H_{QC} = -\frac{1}{\log_2 V}\sum_{i=1}^{V^d}\sum_{j=1}^{V} q_i q_{i,j}\log_2 q_{i,j} \qquad (0 \le H_{QC} \le 1) \tag{16}$$

where H_{QC} is divided by the maximum entropy for the same reason as the curvature entropy.

Figure 13. Extraction of curvature distribution (**a**) Sampling point and a curve unit; (**b**) Sampling of the curvature; (**c**) Quantization based on the curvature; (**d**) Calculation of the transition probability.

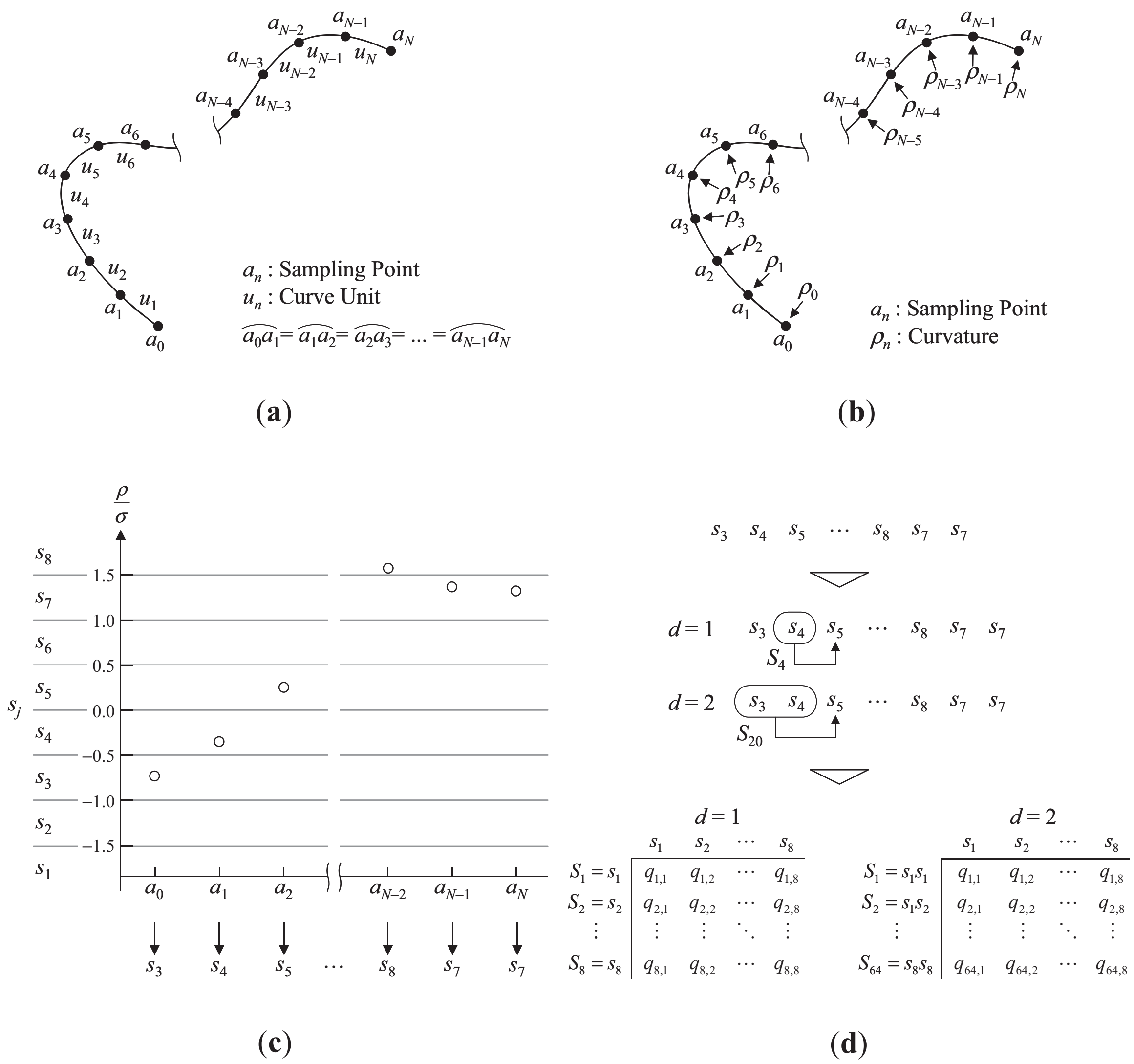

4.2. Relationship between Microscopic Shape Information and Quadratic Curvature Entropy

The relationship between microscopic shape information and quadratic curvature entropy in the curved profiles is analyzed using principal component analysis and in Section 3.3. Due to this analysis, up to the fourth principal components are included in the microscopic shape information whose absolute value of the principal loading exceeds 0.6 (Table 4). The fifth principal component is only included the quadratic curvature entropy. This means that curvature entropy is independent and probably differs from other microscopic shape information.

Table 4. Principal components of shape information.

Shape-information	1st principal component	2nd principal component	3rd principal component	4th principal component	5th principal component
Circumference	**−0.948**	0.119	−0.039	0.094	0.221
Maximum radius vector	**0.878**	−0.083	0.317	−0.273	−0.191
Inclusiveness length	**0.866**	0.003	0.341	−0.296	−0.203
Average width	**0.788**	0.118	0.517	−0.243	−0.179
Roundness	**0.780**	0.048	0.510	−0.300	−0.191
Minimum radius vector	−0.041	**0.973**	−0.080	−0.113	−0.034
X maximum width	−0.430	**0.817**	−0.193	0.315	0.019
Y maximum width	0.466	**0.790**	0.308	0.075	−0.207
Average radius vector	−0.354	0.100	**−0.867**	0.256	0.185
Area	−0.366	0.080	−0.275	**0.869**	0.152
Quadratic curvature entropy	−0.488	−0.179	−0.254	0.190	**0.793**
Contribution ratio (%)	41.374	21.130	16.141	11.767	8.418
Accumulation contribution ratio (%)	41.374	62.504	78.645	90.412	98.830

4.3. Relationship between Shape Information, Including Quadratic Curvature Entropy, and Cognition Information

Similar to the evaluation in Section 3.2, the relationship between shape information and cognition information in curved profiles is evaluated by correlation analysis. The quadratic curvature entropy is highly correlated with the evaluation item of "complex"; the correlation coefficient is higher than that of the curvature entropy (Figure 14).

Figure 14. Relationship between macroscopic shape information and cognition information.

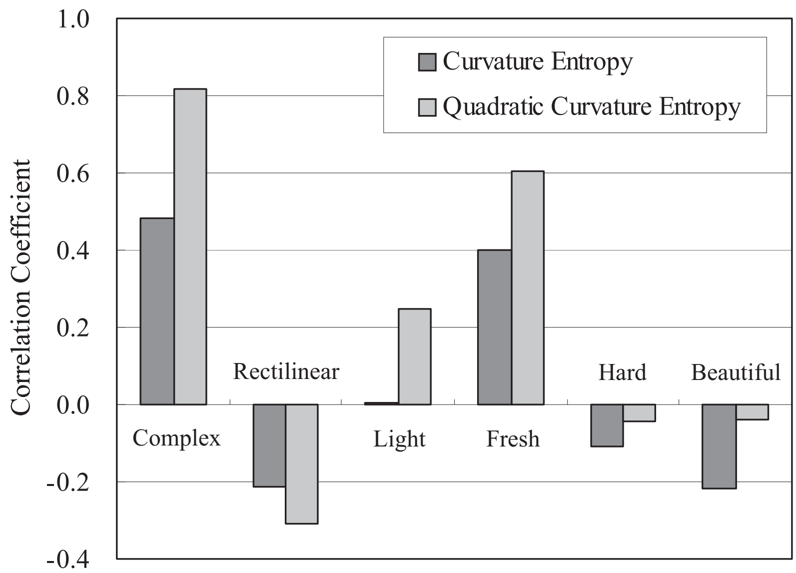

Therefore, the quadratic curvature entropy represents the complexity of a shape in basic curved profiles, and is suitable for shape cognition compared to the curvature entropy. This also means that the continuity of the curvature, which can be evaluated by the quadratic curvature entropy, is important to express macroscopic shape information.

5. Shape Generation Method

5.1. Description of the Initial Shape

In the shape generation method, a three-dimensional Bézier curve is used to describe the initial shape. Herein the side view of an automobile is generated based on conventional studies [25,26]. The side view can be expressed as a polygonal profile consisting of eight basic points (Figure 15a).

Figure 15. Description of the initial shape; (**a**) Basic points; (**b**) Connection points; (**c**) Interpolation by a three-dimensional Bézier curve; (**d**) Movable range of basic points; (**e**) Ruggedness of curve segments; (**f**) Movable range of a tangent vector.

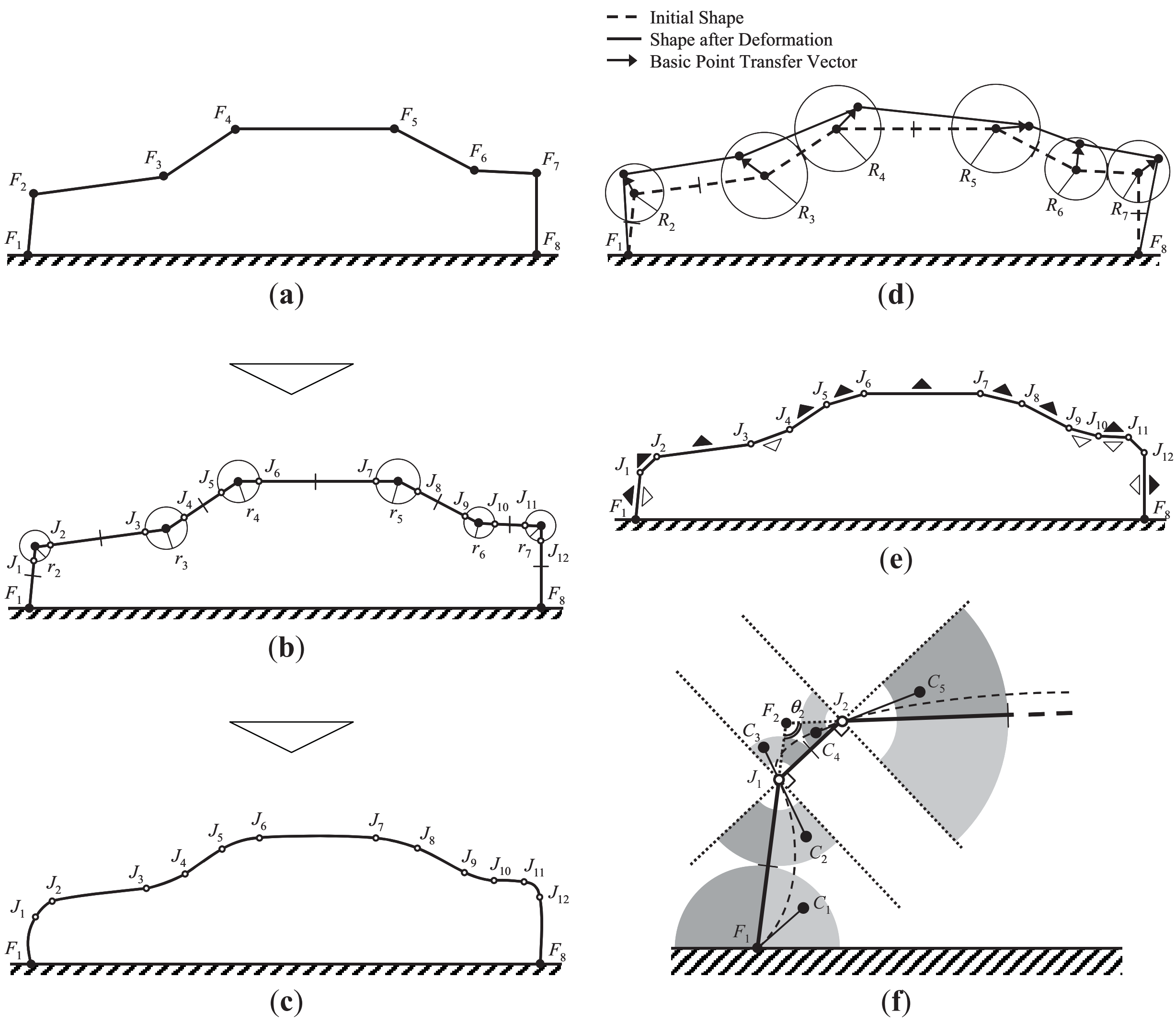

During shape generation, points F_1 and F_8 are fixed, while points F_2 through F_7 are movable. The basic point transfer vector is defined to begin from the basic point toward the deformed points (Figure 15d). The movable ranges of points F_2 through F_7 are defined as circles with radii R_2 through R_7 (Figure 15d). The radii are defined by the following equation:

$$R_k = \frac{1}{2}\min\left\{ \overline{F_{k-1}F_k},\ \overline{F_kF_{k+1}} \right\} \quad (k = 2,3,\ldots,7) \tag{17}$$

This equation prevents shape generation from generating a cross point in a polygonal profile (Figure 16).

Figure 16. Polygonal profile with a cross point.

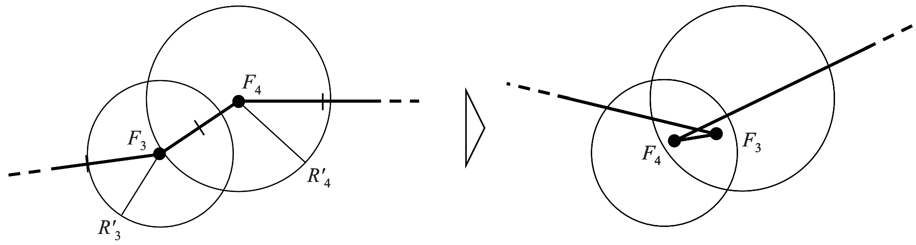

The circles with radii r_2 through r_7 are used to determine the positions of the connection points (Figure 15b). The intersection points between the edges of the circles and the polygonal profile J_1 through J_{12} are used as the connection points. To improve the smoothness of a curved profile, radii r_2 through r_7 are defined as:

$$r_k = \frac{1}{4}\min\left\{ \overline{F_{k-1}F_k},\ \overline{F_kF_{k+1}} \right\} \quad (k = 2,3,\ldots,7) \tag{18}$$

Each segment (F_1 J_1, J_1 J_2, …, J_{12} F_8) is then interpolated using a three-dimensional Bézier curve (Figure 15c).

For shape generation, the initial shape is set to that of the Nissan Bluebird ('99), and the curve control variables (the position of the connection point, direction of a tangent vector, and size of a tangent vector) are set so as to describe this automobile. In the shape generation method, which is illustrated in Figure 15e, the ruggedness (convex or concave) of a curve segment is defined. This means, two control points C_m are placed on the same side of each curve segment for shape generation. To prevent excessive deformation from the initial shape, only the ruggedness of segments F_1 J_1, J_{10} J_{11}, and J_{12} F_8 are selected.

The movable range in the angle of the tangent vector at each connection point is defined as follows (refer to Figure 15f). For differentiable connections, J_1, C_2, and C_3 always form a line, and J_1 C_3 is linked to J_1 C_2. Here, $\angle C_3$ J_1 J_2($<\pi/2$) is calculated as follows when C_2 is on the same side as F_2 :

$$0 < \angle C_3 J_1 J_2 < \frac{1}{2}(\pi - \theta_2) \tag{19}$$

If nothing is present on the same side as F_2, $\angle C_3$ J_1 J_2($< \pi/2$) is calculated:

$$\frac{1}{2}(\pi - \theta_2) < \angle C_3 J_1 J_2 < \frac{\pi}{2} \tag{20}$$

These two definitions prevent shape generation from generating a curved profile with a swell, which can occur in an individual curve segment (Figure 17a) or near a connection point (Figure 17b). The ruggedness of a curve segment is limited by swell prevention (in an individual curve segment) measures, whereas the movable range in the angle of the tangent vector is limited by the swell prevention (around a connection point) measures.

The maximum size of a tangent vector is set to half the length of the segment. This definition prevents shape generation from generating a curved profile with a cross point (Figure 17c). To prevent generating a curved profile with a nondifferentiable connection point, the minimum size is set to 1/3 of the maximum value (Figure 17d).

Figure 17. Swell, cross point, and nondifferentiable point; (**a**) Swell in an individual segment; (**b**) Swell around a connection point; (**c**) Curved profile with cross point; (**d**) Curved profile with a nondifferentiable point.

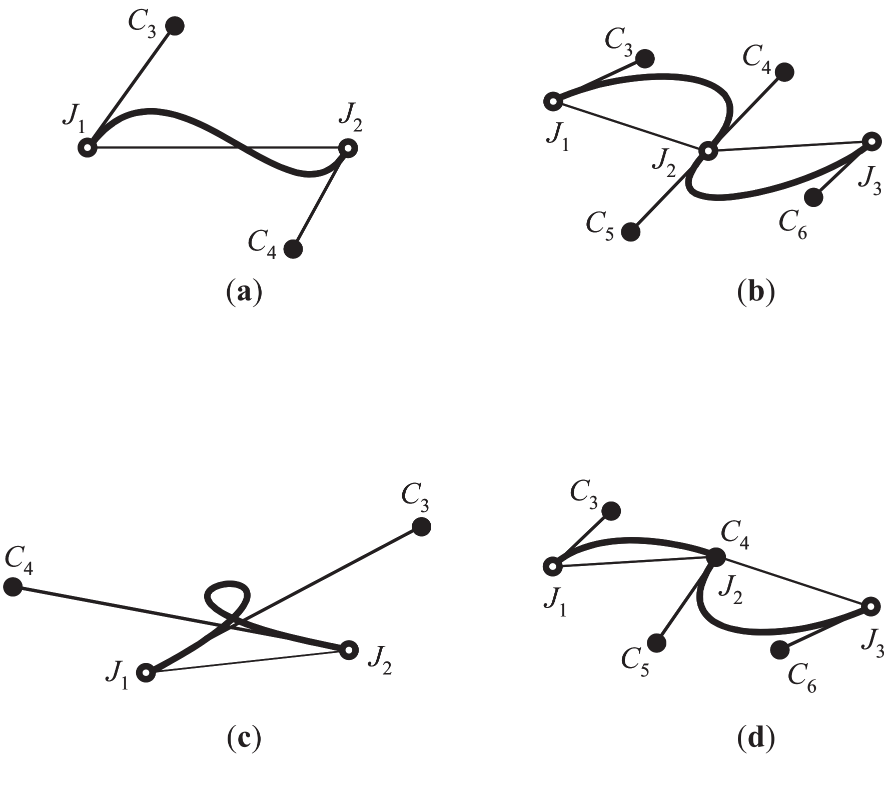

5.2. Coding in a Genetic Algorithm

A genetic algorithm is applied to the shape generation method. The curve control variables (the position of the connection point, direction of a tangent vector, and size of a tangent vector) are defined, and the chromosome for the genetic algorithm is composed of an arrangement of real numbers n_{real} ($0 < n_{\mathrm{real}} < 1$), which adjust the curve control variable as described below.

(1) Position of basic point:

$$x_k = x_{Ik} + n_{\mathrm{real}} w R_k \cos(2\pi\, n_{\mathrm{real}}) \tag{21}$$

$$y_k = y_{Ik} + n_{\text{real}} w R_k \sin(2\pi\, n_{\text{real}}) \tag{22}$$

where w is a degree of freedom in shape generation. x_k and y_k are x and y directional components of the basic point transfer vector, respectively, and x_{Ik} and y_{Ik} are x and y coordinates of the basic point in the initial shape, respectively.

(2) Ruggedness of a curve segment:

If $0 \le n_{\text{real}} < 0.5$, the curve segment is convex. Otherwise ($0.5 \le n_{\text{real}} \le 1 \fallingdotseq$) the curve segment is concave.

(3) Angle of a tangent vector:

n_{real} is used as the ratio for the movable range of the angle (*i.e.*, an angle of the tangent vector is calculated as the product of the range and n_{real}).

(4) Size of a tangent vector:

n_{real} is used as the ratio for the movable range of the size (*i.e.*, a size of the tangent vector is calculated as the product of the range and n_{real}).

The chromosome, which is composed by real numbers n_{real} noted above and used for genetic algorithm, is summarized (Figure 18).

Figure 18. Chromosome.

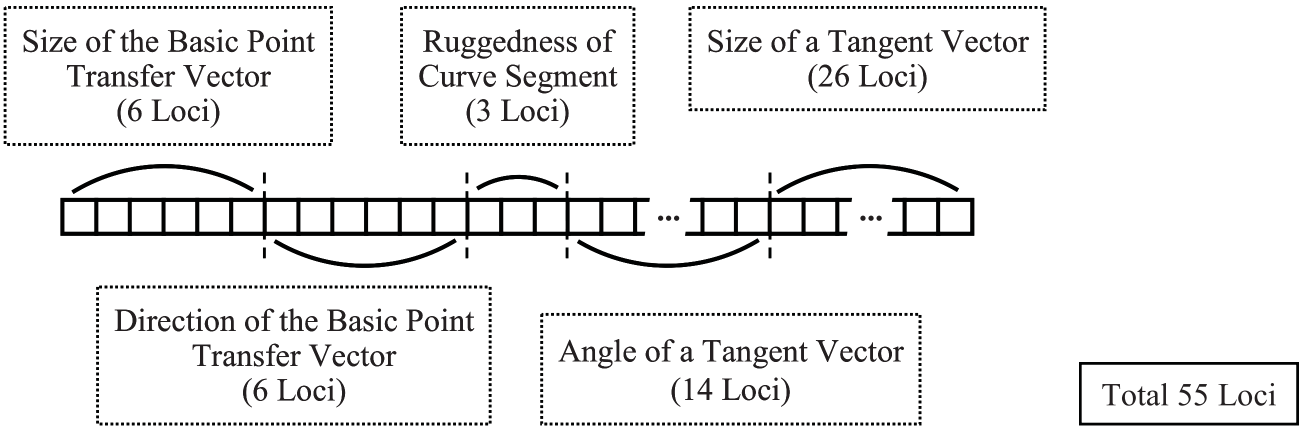

Fitness A is defined as:

$$A = \left|\ H_{CD} - \left(H_{CI} + \Delta H_C\right)\ \right| \tag{23}$$

where H_{CI} is the curvature entropy of the initial shape, H_{CD} is the curvature entropy of the phenotype (shape after deformation), and ΔH_C is the variation in the curvature entropy set by the designer. A shape with fitness $A < 0.01$ is derived as a design candidate.

Using the quadratic curvature entropy, Equation (23) is transformed into the following equation:

$$A = \left|\ H_{QCD} - \left(H_{QCI} + \Delta H_{QC}\right)\ \right| \tag{24}$$

where H_{QCI} is the quadratic curvature entropy in the initial shape, H_{QCD} is the quadratic curvature entropy in the phenotype, and ΔH_{QC} is the target variation of the quadratic curvature entropy. The crossover and mutation are conducted in the same manner described in a conventional study [27]. The random weighted mean of the real number variable is used for the crossover and mutation rate is set to 20%. The elite saving strategy and tournament selection are used for the selection. The population size (number of the combination of chromosomes) is set to 20. Figure 19 shows the flow of the search algorithm.

Figure 19. Search algorithm.

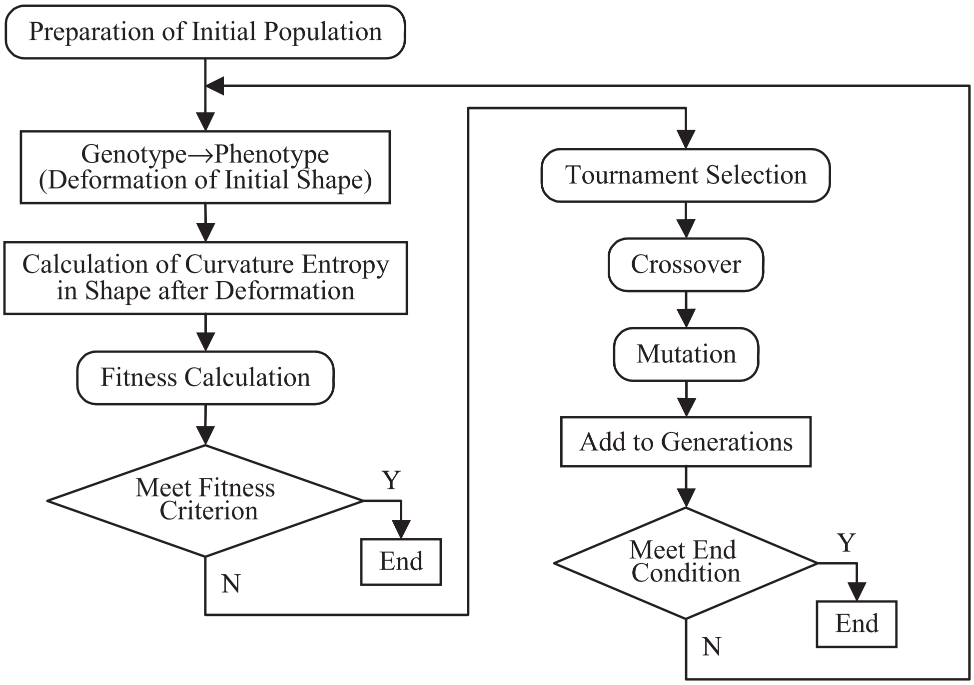

6. Application of Shape Generation Method

6.1. Description of the Initial Shape and Conditions in the Genetic Algorithm

The degree of freedom in the shape generation w is set to three (0.5, 0.75, and 1). To search an adequate number of curve units N, the curvature entropy of the initial shape H_{CI} with respect to the change in the number of curve units is calculated (Figure 20).

Figure 20. Relationship between the curvature entropy and the number of curve units.

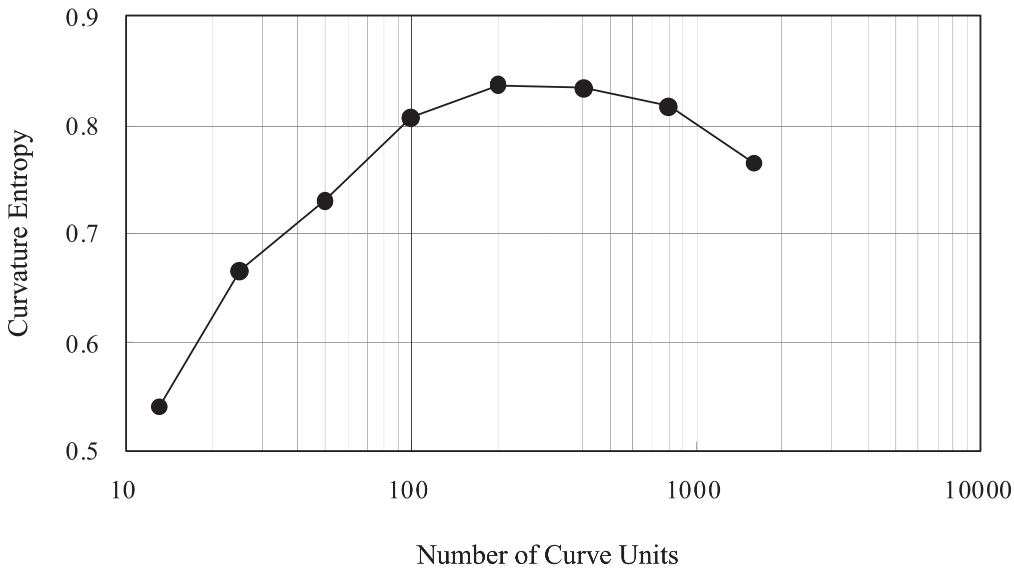

Consequently, the curvature entropy peaks at $N = 200$ (*i.e.*, N should be set to 200 for the higher degree of freedom in the shape generation).

The shape generation method is executed using each of the three aforementioned constraints, and the variation ranges of the curvature entropy H_C and quadratic curvature entropy H_{QC} are calculated as the average of 10 shape generations. As shown in Figure 21, the variation range for each is approximately 0.12. To compare shape generation under the same conditions, the variations of curvature entropy ΔH_C and quadratic curvature entropy ΔH_{QC} are set ±0.12 and ±0.06.

Figure 21. Variation ranges of the curvature entropy and quadratic curvature entropy.

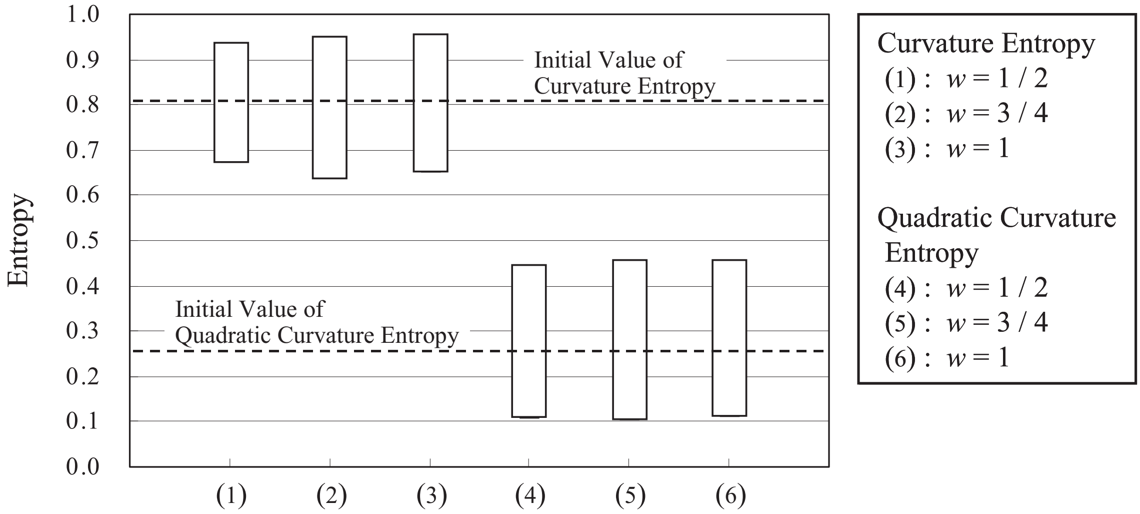

6.2. Shape Generation and Cognition Experiment

Figure 22 shows examples of the generated shapes. The specifications of a cognition experiment using the generated shapes as samples are as follows:

Figure 22. Examples of the generated shapes.

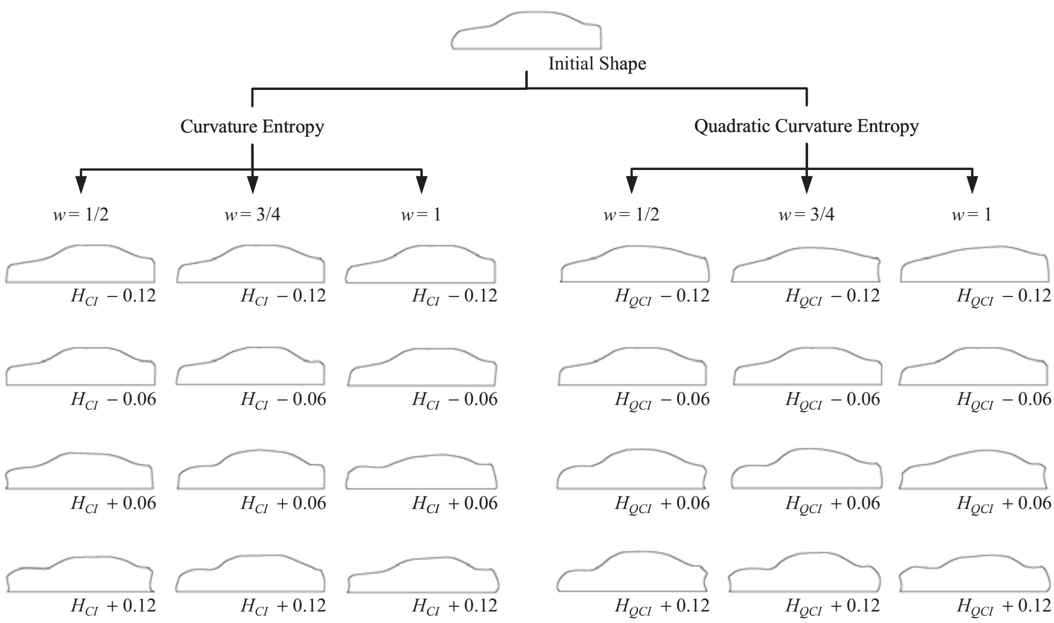

(1) Method: semantic differential method (5 stages)
(2) Samples: generated shapes (10 samples for each condition-type of macroscopic shape information, w, and ΔH)
(3) Evaluation item: "complex"
(4) Examinees: 13 students in their early 20 s

As shown in Figure 23, samples are presented on a PC monitor. The generated shapes with either variation in the curvature entropy ΔH_C (= −0.12, −0.06, +0.06 or +0.12) or quadratic curvature entropy ΔH_{QC} (= −0.12, −0.06, +0.06 or +0.12) are randomly placed, except the initial shape, which is in the center.

Figure 23. Presentation of the samples.

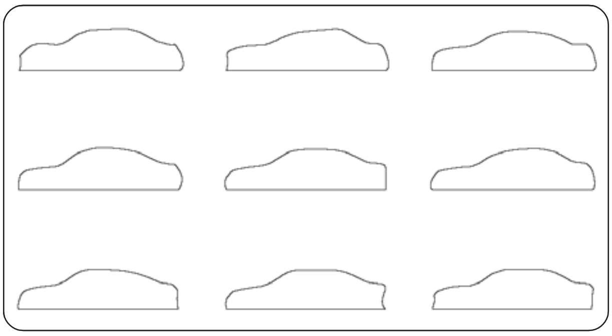

6.3. Relationship between Macroscopic Shape Information and Cognition Information

The correlation between the cognition information (as a purpose variable) and the curvature entropy (as an explanatory variable) is analyzed. As shown in Figure 24, the correlation coefficient between the quadratic curvature entropy and cognition information (complexity) exceeds 0.8 regardless of the degree of freedom in the shape generation. On the other hand, the correlation coefficient between the curvature entropy and complexity decreases according to the degree of freedom of shape generation. The significance levels for all conditions are less than 0.01.

Figure 24. Relationship between the degree of freedom in shape generation and the correlation coefficient.

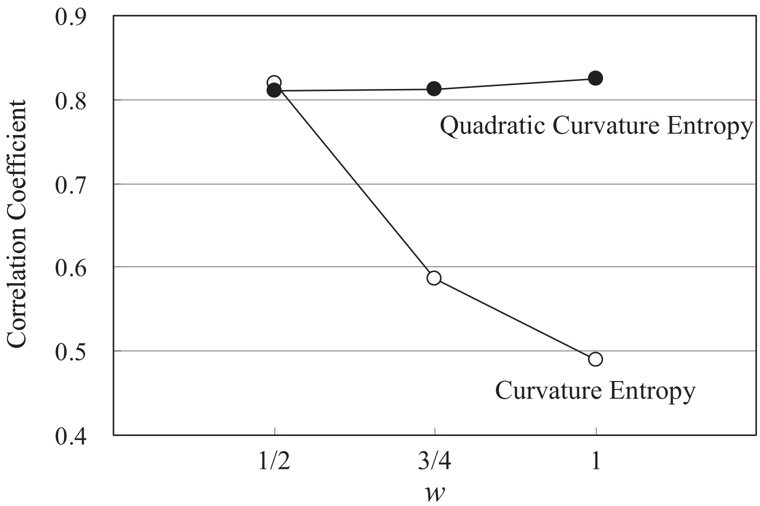

The results demonstrate that the curvature entropy and quadratic curvature entropy represent complexity not only in a basic curved profile, but also in the shape of the products, such as the side view of an automobile. Moreover, in case of a higher degree of freedom in shape generation, the correlation coefficient between complexity and curvature entropy decreases, which is likely due to the fact that the continuity of curvature is not considered. Therefore, consideration of the curvature continuity in the definition of macroscopic shape information in adjustable shape cognition is important.

7. Conclusions

This study defines macroscopic shape information (curvature entropy) to provide a useful design index for curved surface designs. For a basic curved profile, curvature entropy can represent the complexity of a shape, which is difficult to represent with conventional microscopic shape information. In addition, the introduction of the Markov process, which effectively approximates the evaluation of human cognition, to consider the curvature continuity improves the curvature entropy. The improved curvature entropy (quadratic curvature entropy) is confirmed to represent the complexity and to favorably approximate the human cognition compared to the curvature entropy.

A shape generation method using curvature entropy and quadratic curvature entropy is developed and applied to the side view design of an automobile. The macroscopic shape information can represent the complexity of an automobile. Moreover, the quadratic curvature entropy based on a Markov process is effective regardless of the parameter in the shape generation method. In other words, the quadratic curvature entropy may accommodate various applications.

Figure 25 shows an image of a curved surface design support system based on the knowledge acquired in the present study. The flow of shape generation in this system is described below. First designers describe the initial shape based on a conventional side view of an automobile (Figure 25a). Then this system automatically generates a shape based on the variation of entropy set by the designers. Finally, the designers select one of the generated shapes after considering other factors (Figure 25b) and generate a three-dimensional model based on the selected shape (Figure 25c). Because the designers can control the complexity of the generated shape, the shape generation method described herein can support designers during the early stage, which is when the designers must decide the overall impression of the design.

Future tasks include:

(1) Validating the method constructed in this study for other shapes such as natural/geometric shapes and not just basic curved profiles.
(2) Evaluating the relationship between the cognition of the complexity and scale dealt with in the field of CSS (Curvature Schale Space).
(3) Comparing the genetic algorithm to other methods that search for curved profiles by changing the curved control variables.

Figure 25. Curved surface design support system. (**a**) Description of the initial shape; (**b**) Shape generation and selection; (**c**) Generation of the three-dimensional model.

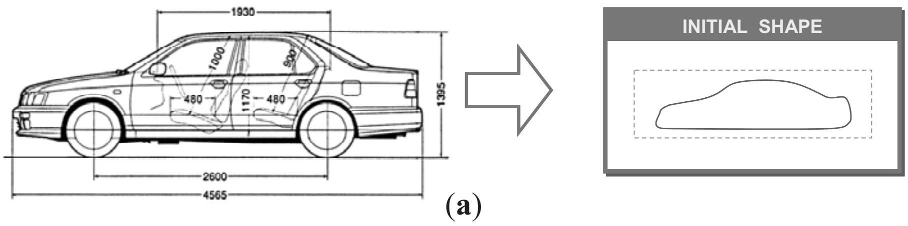

(**a**)

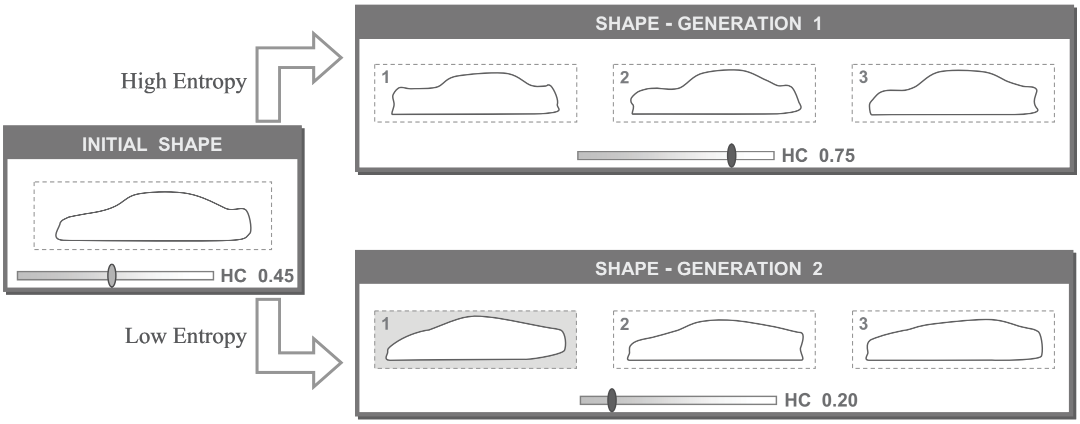

(**b**)

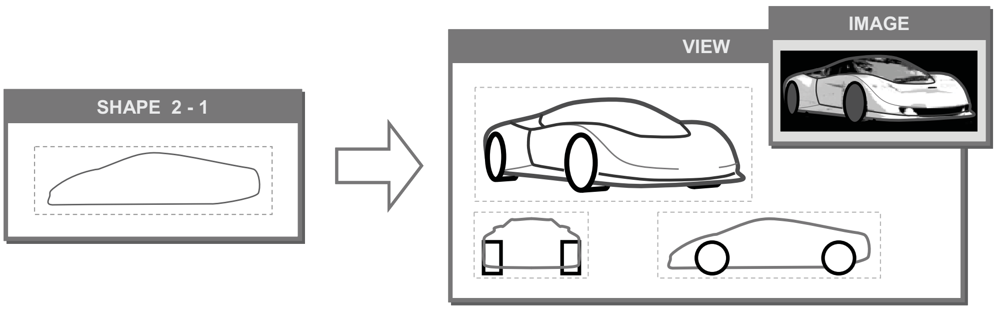

(**c**)

Acknowledgments

This work was supported in part by a Grant-in-Aid for the Global Center of Excellence Program for "Center for Education and Research of Symbiotic, Safe and Secure System Design" from the Ministry of Education, Culture, Sports, Science and Technology of Japan.

References and Notes

1. Metzger, W. *Gesetze des Sehens*, 2nd ed.; Kramer: Frankfurt, Germany, 1953.
2. Beck, J. Effect of orientation and of shape similarity on perceptual grouping. *Percept. Psychophys.* **1966**, *1*, 300–302.
3. Beck, J. Perceptual grouping produced by changes in orientation and shape. *Science* **1966**, *154*, 538–540.
4. Polanyi, M. *The Tacit Dimension*; Routledge & Kegan Paul Ltd.: London, UK, 1966.

5. Kanizsa, G. Subjective contours. *Sci. Am.* **1976**, *234*, 48–52.
6. Kuyama, H. Measurements of feature-parameters of signs. *Science of Design* **1998**, *45*, 35–44.
7. Asada, H.; Brady, M. The curvature primal sketch. *IEEE Trans. Pattern. Anal. Mach. Intell.* **1986**, *8*, 2–14.
8. Mokhtarian, F.; Mackworth, A.K. Scale-based description and recognition of planar curves and two-dimensional shapes. *IEEE Trans. Pattern. Anal. Mach. Intell.* **1986**, *8*, 34–43.
9. Mokhtarian, F.; Mackworth, A.K. A theory of multiscale, curvature-based shape representation for planar curves. *IEEE Trans. Pattern. Anal. Mach. Intell.* **1992**, *14*, 789–805.
10. Mokhtarian, F. Silhouette-based isolated object recognition through curvature scale space. *IEEE Trans. Pattern. Anal. Mach. Intell.* **1995**, *17*, 539–544.
11. Harada, T.; Yoshimoto, F.; Moriyama, M. An aesthetic curve in the field of industrial design. In Proceedings of the 1999 IEEE Symposium on Visual Language, Tokyo, Japan, 13–16 September 1999; pp. 38–47.
12. Harada, T.; Mori, N.; Sugiyama, K. Study of quantitative analysis of curve's character. *Science of Design* **1994**, *40*, 9–16.
13. Harada, T.; Mori, N.; Sugiyama, K. Algorithm of creating the curve by controlling its characteristics. *Science of Design* **1994**, *41*, 1–8.
14. Jernigan, M. E.; D'Astous, F. Entorpy based texture analysis in the spatial frequency domain. *IEEE Trans. Pattern. Anal. Mach. Intell.* **1984**, *6*, 237–243.
15. Thiran, P.; Crounse, R.K.; Chua, O.L.; Hasler, M. Pattern formation properties of autonomous cellular neural networks. *IEEE Trans. Circuits. Syst. I* **1995**, *42*, 757–774.
16. Ujiie, Y.; Matsuoka, Y. Shape-generation method using curvature entropy. In Proceedings of the 2000 ASME International Mechanical Engineering Congress and Exposition, Orlando, FL, USA, 5–10 November 2000; pp. 85–92.
17. Shannon, C.E.; Weaver, W. *The Mathematical Theory of Communication*; The University of Illinois Press: Chicago, IL, USA, 1964.
18. Blahut, R.E. *Principles and Practice of Information Theory*; Addison-Wesley Publishing Company: Boston, MA, USA, 1987.
19. Ujiie, Y.; Matsuoka, Y. Macro-informatics of cognition and its application for design. *Adv. Eng. Informat.* **2009**, *23*, 184–190.
20. Birkhoff, G.D. *Aesthetic Measure*; Harvard University Press: Cambridge, UK, 1933.
21. Miura, M.; Sugihara, T.; Kunifuji, S. GKJ: Group KJ method support system utilizing digital pens. *IEICE Trans. Info. Syst.* **2011**, *E94-D*, 456–464.
22. Hosaka, M. *Modeling of Curves and Surfaces in CAD/CAM*; Springer-Verlag: Berlin, Germany, 1992.
23. Yamaguchi, F. *Curves and Surfaces in Computer Aided Geometric Design*; Springer-Verlag: Berlin and Heidelberg, Germany, 1988.
24. Suzuki, T.; Asanuma, T.; Matsuoka, Y. The proposal of the macroscopic design information as a shape design index. In Proceedings of the 4th Asian Design Conference, Nagaoka, Niigata, Japan, 30–31 October 1999; pp. 214–221.
25. Tian, M.; Sugiyama, K.; Kamaike, M.; Watanabe, M. A car form generation system based on evolutionary computation. *Science of Design* **1997**, *44*, 77–86.

26. Tian, M.; Sugiyama, K.; Kamaike, M.; Watanabe, M.; John, S. A design support system based on co-evolutionary process. *Science of Design* **1998**, *45*, 65–74.
27. Obayashi, S. Aerodynamic design and inverse problem. *Science of Design* **1996**, *1*, 21–27.